Intersubband transitions in InAs/AlSb quantum wells

A. Simon, J. Scriba, C. Gauer, A. Wixforth and J. P. Kotthaus
Sektion Physik, Ludwig-Maximilians-Universität, 8000 München 22 (Germany)
C. R. Bolognesi, C. Nguyen, G. Tuttle and H. Kroemer
Department of Electrical and Computer Engineering, University of California, Santa Barbara, CA 93106 (USA)

Abstract

Collective intersubband resonances in InAs/AlSb single quantum wells are studied in terms of their dependence on the well width and the electron density. The transitions are found to lie within the atmospheric windows of 8–12 μm and 3–5 μm, respectively.

Optical detectors and modulators based on intersubband transitions have been widely discussed since the first experimental observation of such transitions in GaAs quantum wells [1]. So far, the experiments and theoretical investigations have concentrated on GaAs/AlGaAs heterostructures, for a recent review see ref. 2. In this system, device parameters for detector applications matching those of commercially available HgCdTe or InSb detectors [3] have been demonstrated. There are, however, a number of drawbacks of GaAs/AlGaAs quantum wells inherent in their bandstructure, such as a limited spectral range. Therefore efforts have been made to grow material systems which combine the mature processing technology of III-V semiconductors with a band alignment allowing for detectors with a larger frequency range.

InAs quantum wells stacked between AlSb barriers represent such a novel heterostructure. The electrically active layers are grown on GaAs substrates so that GaAs technology can be used to integrate the structures. Despite a lattice mismatch of about 7% between the active layers and the substrate, low temperature mobilities reach values as high as 800 000 $cm^2\ V^{-1}\ s^{-1}$. The effective electron mass of InAs is only 0.023 m_0 and the AlSb barriers have a height of 2.1 eV at the Γ point, so that large subband quantization energies are expected. The oscillator strength of the intersubband transition is also larger than in the case of GaAs/AlGaAs, since it is proportional to the inverse of the effective mass [1]. Excitations from higher subbands with even greater transition probabilities can be realized because high electron densities, on the order of 5×10^{12} cm^{-2}, are readily achieved [4]. The origin of the electrons in such not intentionally doped structures is discussed in ref. 5. Another interesting feature of the system is that the subband spacing of narrow wells may become larger than the band gap, so that the advantages of an intersubband- and interband-detector may be combined in the same device.

Here we report on the observation of intersubband resonances (ISR) in InAs/AlSb quantum wells. Samples with well widths of 150, 120, 96 and 82 Å are investigated. The layer sequence is as follows: on top of a GaAs substrate a sequence of buffer layers is grown as described in ref. 6; the InAs quantum well is clad by two 200 Å AlSb barriers, and a 50 Å GaSb cap layer terminates the growth sequence.

To induce intersubband transitions the incident light should be polarized along the direction of confinement. We use the strip line geometry to realize this polarization and to enhance the signal by multiple passes through the sample [7]. The top of the sample is metallized so that it can serve as a gate electrode and ensures an electric field component perpendicular to the two-dimensional electron gas (2DEG). The back of the sample is polished in order to minimize losses caused by diffuse scattering from the surface. Our sample geometry is shown as an inset to Fig. 1.

All experiments are carried out in a low-temperature cryostat containing a superconducting solenoid providing a maximum field of 15 T. The far-infrared spectra are taken with a rapid-scan Fourier transform spectrometer. Experimentally, we determine the relative change in transmisssion $-\Delta T/T=(T-T_0)/T_0$, where T_0 denotes the transmission of a reference spectrum, taken either at a different carrier density or at a different magnetic field.

In Fig. 1 we show relative transmittance spectra measured at different gate voltages, *i.e.* carrier densities, in a quantum well 150 Å wide. The reference spec-

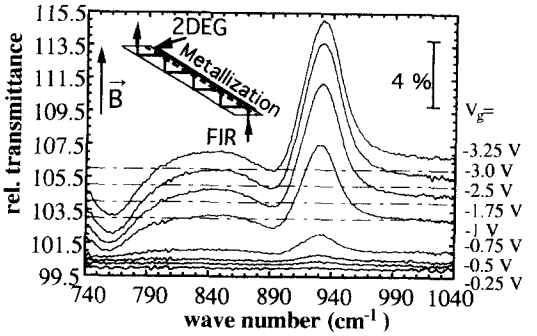

Fig. 1. Relative change of the infrared transmission taken at different carrier densities. The inset shows the experimental geometry.

trum is taken at $V_g = 0$ V. The carrier density in these structures cannot be tuned by simply evaporating a Schottky gate directly on top. Therefore we deposit a 1500 Å silicon layer before evaporating the gate electrode. It is found in Shubnikov-de Haas measurements that the number of carriers in this sample is reduced by about 20% at $V_g = -3.25$ V as compared to $V_g = 0$ V. As the electron density decreases with more negative gate bias, a peak in the relative transmission (caused by the absorption in the reference spectrum) at about 930 cm^{-1} gains strength. On the low-energy side a dip appears and deepens with decreasing carrier density. For gate voltages smaller than $V_g \leqslant -1$ V an additional minimum arises at about 760 cm^{-1}.

Tuning the electron density modifies the spectra in two ways. The absorption is proportional to the number of carriers, so that weak absorption is expected when the carrier density is low. Furthermore, many-body effects such as the depolarization and the exciton shift depend on the carrier density [8]. Finally, the self-consistent potential and effects caused by the non-parabolicity of the InAs conduction band both influence the transition energy and the line shape of the resonance [9]. The prominent peak found at $V_g < -0.5$ V is thus identified as being induced by the intersubband transition at the highest carrier density at $V_g = 0$. The dip on the low-energy side of this maximum is an artefact caused by the division of two spectra of different line shapes. A similar effect will be discussed in detail in the next paragraph. Because of the silicon layer between the metal gate and the sample, the parallel component of the infrared electric field in the plane of the quantum well is finite, so that in this setup parallel-excited intersubband absorption may be detected [10]. This excitation mechanism is found in the intersubband resonance on non-parabolic semiconductors, and its oscillator strength is approximately 10% of the perpendicular excitation under the same experimental conditions [11]. We thus interpret the minimum at around 760 cm^{-1} as the parallel-excited intersubband transition. The energetic difference between the two excitation mechanisms is mainly determined by the depolarization shift $E_{dep} = E_{12\perp} - E_{12\parallel}$. Calculating the depolarization effect for an infinitely high square well gives a shift of $E_{dep} = 140$ cm^{-1}, which is in good agreement with the one determined experimentally.

We now focus on the spectra obtained from the magnetic field ratio. In these experiments the magnetic field is oriented at an angle of 45° with respect to the sample, as shown in the inset to Fig. 1. Dividing the spectra at $B \neq 0$ T by the reference spectrum measured at $B = 0$ T gives the relative spectra in Fig. 2 for the same 150 Å wide quantum well. In these plots the strength of the relative signal increases non-linearly with the strength of the magnetic field. The spectrum at 15.3 T exhibits a prominent peak at about 910 cm^{-1} and two minima on either side. This signature is also seen in the 12 T spectrum, even though not that pronounced. The structure of the spectra taken at lower fields exhibits a minimum at high energies and a maximum at low energies. The positions of these extrema shift with the variation of the magnetic field.

In tilted magnetic fields the electric and magnetic quantizations are coupled, for a recent review see ref. 12. The component of the magnetic field $B_\parallel$ parallel to the 2DEG induces a diamagnetic shift on the subband energies

$$E_{n,dia} = \frac{e^2 B_\parallel^2}{2m^*}\left[(z_{nn}^2) - (z_{nn})^2\right] \qquad (1)$$

Here, z_{nn} denotes the matrix element defined by

$$(z^x)_{ij} = \int dz \phi_i z^x \phi_j$$

whereas the other symbols have their usual meaning. Furthermore, in parallel magnetic fields the subband separation depends on k_x:

$$E_{10}(k_x) = E_{10} + \frac{e^2 B_\parallel^2}{2m^*}\left[(z_{11}^2) - (z_{00}^2)\right] + \frac{\hbar e B_\parallel}{m^*} k_x (z_{11} - z_{00})$$

According to eqn. (1) the component $B_\parallel$ influences the energy of the second subband more strongly than the energy of the first. Thus the division of two spectra taken at different magnetic fields results in a relative spectrum as shown in Fig. 2. The maxima are related to the intersubband transition at $B = 0$ T while the minima are caused by the absorption at $B \neq 0$ T. The non-linear variation of the signal with the magnetic field can be explained by the B^2 dependence of the diamagnetic shift and the division of the spectra. To study the line shape of the spectra in detail, we calculate the real part of the dynamic conductivity given by

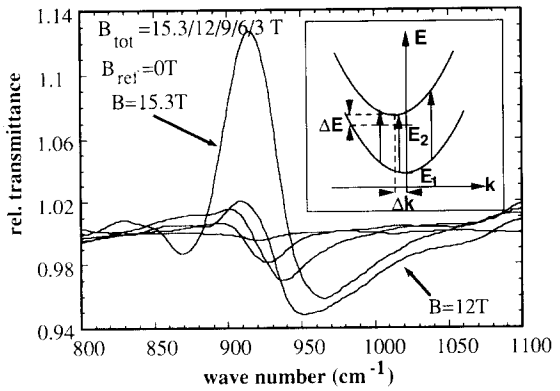

Fig. 2. Relative change of the infrared transmission taken at different magnetic fields. Note that the position of the maximum of the spectrum $B = 15.3$ T / 0 T approximately coincides with the maximum of the spectrum taken at $V_g = 0$ and $B = 0$ T in the density ratio. The inset shows the shift of the subband parabolae caused by the in-plane component of the magnetic field.

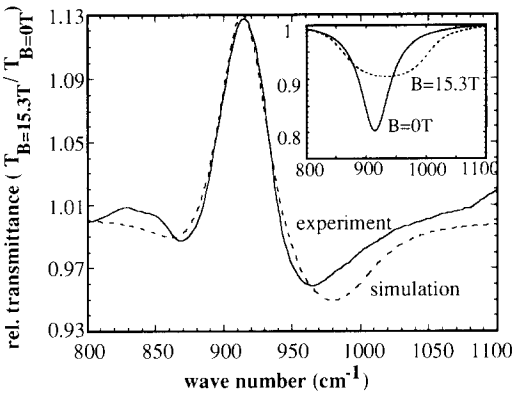

Fig. 3. Fit to the spectrum 15.3 T / 0 T. The curves in the inset represent the line shape of the resonances as obtained by fitting the dynamic conductivity to the relative spectrum.

ref. 13:

$$\mathrm{Re}(\sigma_{zz}(\omega)) = A\frac{\omega^2}{\tau}\sum_{-k_F}^{+k_F}\frac{1}{\left(\hbar^2\omega^2 - \frac{\hbar^2}{\tau^2} - E_{12}^2(k)\right)^2 - \frac{4\hbar^2\omega^2}{\tau^2}}$$

The resonance curves shown in Fig. 3 are obtained by adjusting the oscillator strength, linewidth and transition energy to the relative spectrum at 15.3 T / 0 T. As can be seen, the calculated resonance at $B = 15.3$ T is shifted to higher energies and it is considerably broader than the resonance at $B = 0$. We also simulate the spectra of the narrower wells with the same fit. The single-particle intersubband spacings for the four different InAs quantum well widths are approximated by subtracting the depolarization shift as calculated for an infinitely high square well. According to ref. 9 the exciton shift may be neglected in this calculation. The values deduced from the ISR measurements deviate only negligibly from the values derived from cyclotron resonance measurements in tilted magnetic fields [14] that will be described elsewhere. Table 1 lists the values of ISR and E_{12} energies extracted for the four different InAs quantum well widths, along with the corresponding 2DEG concentrations N_s.

In summary, we have measured bound-to-bound intersubband transitions in single InAs quantum wells demonstrating the wide frequency range (113–246 meV) that can be attained in such heterostructures. So far, no theoretical approach for calculating the subband energies in strongly non-parabolic systems gives subband separations in quantitative agreement with the experiment. Our experiments prove that InAs/AlSb quantum wells indeed offer great promise as novel infrared detectors.

TABLE 1. Intersubband resonances, E_{12} energies and 2DEG concentration (N_s) values for different InAs quantum well widths

Well width (Å)	ISR (cm^{-1})	E_{12}[a] (cm^{-1})	N_s (10^{12} cm^{-2})
150	910	770	1.5
120	1360	980	1.0
96	1680	1630	0.7
82	1980	1960	0.4

[a]The single particle level spacings E_{12} are derived from the experimentally determined transition energies by subtracting the depolarization shift calculated for an infinitely high square well.

Acknowledgments

We gratefully acknowledge financial support from the Volkswagen Stiftung. The work in Santa Barbara was supported in part by the Offfice of Naval Research, in part by QUEST, the NSF Science and Technology Center for Quantized Electronic Structures (Grant DMR 91-20007).

References

1 L.C. West and S.J. Eglash, *Appl. Phys. Lett., 46* (1985) 1156.
2 E. Rosencher *et al.* (eds.), *Intersubband Transitions in Quantum Wells*, Plenum Press, New York, 1992.
3 S.C. Shen, *Semicond. Sci. Techn., 8* (1993) 400.
4 4 C. Nguyen, B. Brar, C.R. Bolognesi, J.J. Pekarik and J.H. English, *J. Electron. Mater., 22* (1993) 255.
5 C. Nguyen, B. Brar, H. Kroemer and J.H. English, *J. Vac. Sci. Technol. B, 10* (2) (1993) 898.
6 G. Tuttle, H. Kroemer and J.H. English, *J. Appl. Phys., 65* (1989) 5239.
7 P. Kneschaurek, A. Kamgar and J.F. Koch, *Phys. Rev. B, 14* (1976) 1610.

8 T. Ando, A.B. Fowler and V. Stern, *Rev. Mod. Phys., 54* (1982) 473.
9 M. Zaluzny, *Phys. Rev. B, 47* (1993) 3995.
10 M. von Ortenberg, *Infrared Physics, 18* (1978) 735.
11 W. Zawadzki, *J. Phys. C, 16* (1983) 229.
12 E. Batke, *Festkörperprobleme, 31* (1991) 297.
13 J. Scriba, *Doctoral Thesis*, Ludwig-Maximilians-Universität München, 1993 (unpublished).
14 S. Oelting, A.D. Wieck, E. Batke and U. Merkt, *Surf. Sci., 196* (1986) 273.